High-Pressure Carbon Monoxide Adsorption on Pt(111) Revisited: A Sum Frequency Generation Study†

G. Rupprechter,* T. Dellwig, H. Unterhalt, and H.-J. Freund

Fritz-Haber-Institut der Max-Planck-Gesellschaft, Chemical Physics Department, Faradayweg 4-6, D-14195 Berlin, Germany

Received: October 2, 2000; In Final Form: January 8, 2001

The adsorption of CO on Pt(111) was studied by picosecond infrared−visible sum frequency generation (SFG) vibrational spectroscopy in a pressure range from 10^{-7} to 500 mbar and in a temperature range of 160−400 K. At low pressure the experiments were complemented by TPD, LEED, and AES. Terminally bonded (on-top) CO was the only species observed between 160 and 400 K, independent of gas pressure. The CO stretching frequency was blue-shifted by about 15 cm^{-1} with increasing pressure (up to 2097 cm^{-1}), but no evidence for high-pressure CO species or surface roughening was found. The influence of defects was also investigated. CO adsorption on a defective (nonannealed) Pt(111) surface yielded peaks that were slightly broadened but otherwise identical to the defect-free surface. At 160 K, a second peak at 2085 cm^{-1} evolved above 50 mbar of CO. TPD revealed that under these conditions residual (contaminant) water adsorbs on the surface. The coadsorption of water and CO red-shifted the terminal CO peak by about 15 cm^{-1}, resulting from the substrate-mediated interaction of CO and water.

1. Introduction

The adsorption system carbon monoxide on Pt(111) is undoubtedly the "*Drosophila*" of surface science. The enormous interest in this system originates from its relevance to catalysis, since CO takes part in many important reactions (CO hydrogenation and oxidation, Fischer−Tropsch synthesis, car emission control) and Pt is among the most frequently used active metals (petroleum processing, ammonia oxidation, etc).[1−3] Furthermore, CO is a perfect probe molecule to study adsorption by vibrational spectroscopy [e.g., by high-resolution electron energy loss spectroscopy (HREELS) and infrared reflection absorption spectroscopy (IRAS)], temperature-programmed desorption (TPD), and a variety of other methods (a historical account was given by John T. Yates, Jr.).[4] Since CO can adopt different adsorption geometries (terminal, 2-fold bridging, 3-fold hollow), it provides information about the surface site distribution. Pt(111) can be easily prepared and even the clean surface exhibits remarkable properties such as relaxation and reconstruction.[2] The ease of handling CO and Pt(111) in an ultrahigh vacuum-(UHV-) based surface analysis chamber gives another credential to this combination.

Although a wealth of information was obtained under UHV conditions, the extrapolation of these data to catalytic reaction conditions ≥1 bar was frequently questioned. Consequently, the development of surface-sensitive techniques that can work around atmospheric pressure rejuvenated the interest in CO/Pt(111), because these methods allow in situ studies in a high-pressure environment and a comparison between UHV and atmospheric conditions. Somorjai and co-workers studied the adsorption of CO on Pt(111) by high-pressure scanning tunneling microscopy (HP-STM)[5] and sum frequency generation (SFG) spectroscopy.[6] Above 15 mbar of CO pressure, the fraction of on-top CO decreased at 300 K and Pt−carbonyls (around 2050 cm^{-1}) and an incommensurate CO overlayer were formed. These species that only appeared at high pressure were also observed during subsequent studies of CO oxidation.[7,8] In the case of Pt(110), pronounced surface rearrangements were monitored in CO, O_2, and H_2 by HP-STM.[9] Härle et al.[10] applied SFG spectroscopy to study CO chemisorption on polycrystalline Pt foil up to atmospheric pressure. At 300 K, the on-top CO peak strongly decreased above 10 mbar (but was detectable up to 300 mbar) and a new "low-frequency" CO surface species appeared above 50 mbar of CO. However, the SFG signal from the low-frequency species was very small (about 2% of the on-top CO signal). In both articles[6,10] the low-frequency spectral features were attributed to the formation of Pt−carbonyl complexes resulting from a displacive reconstruction of Pt atoms at high CO pressure.

In light of these observations, we have revisited CO/Pt(111) using our new SFG-compatible UHV−high-pressure reaction cell (see section 2.2).[11,12] In our study terminal CO was the only species observed between 10^{-7} and 500 mbar and between 160 and 400 K. On-top CO was stable under the conditions studied, and pressure-dependent changes only occurred in the presence of coadsorbed water at 160 K, which led to a red shift of terminal CO. High-pressure SFG studies on alumina-supported Pd nanoparticles, carried out recently with the same equipment, were published elsewhere.[11]

2. Experimental Section

2.1. Sum Frequency Generation Spectroscopy. Optical infrared−visible sum frequency generation allows one to obtain vibrational spectra of adsorbates from submonolayer coverages (UHV) to ambient pressure. Since SFG uses photons to probe adsorbate vibrations, the need of a vacuum environment that limits electron spectroscopies (e.g., HREELS) does not apply. The surface specificity of SFG or, in other words, the insensitivity of SFG to the gas phase allows acquisition of surface spectra

† Part of the special issue "John T. Yates, Jr. Festschrift".

* Corresponding author: e-mail rupprechter@fhi-berlin.mpg.de; phone +49 30 8413 4132; fax +49 30 8413 4105.

10.1021/jp003585s CCC: $20.00 © 2001 American Chemical Society
Published on Web 03/13/2001

even at high gas pressures. SFG spectroscopy has been reviewed several times[10,13−15] and we will therefore focus on aspects that are relevant to the present study.

To acquire an SFG vibrational spectrum of CO on Pt(111), two picosecond laser pulses are spatially and temporally overlapped on the sample. The visible beam is held at fixed frequency (ω_{vis}), while the infrared beam (ω_{IR}) is frequency-tuned to probe the vibrational modes of CO. When the IR energy excites a vibrational resonance, photons are emitted with a frequency equal to the sum of the two input photon frequencies ($\omega_{SFG} = \omega_{IR} + \omega_{vis}$), i.e., in the visible region. By tuning the IR beam and monitoring the SFG intensity, a vibrational spectrum can be obtained by plotting the SFG intensity vs the IR energy. However, for a vibrational mode to be SFG-active it must satisfy both infrared and Raman selection rules, due to the second-order nonlinearity of SFG. Consequently, SFG is only allowed in media without inversion symmetry, e.g., at surfaces where the inversion symmetry is broken (in the electric dipole approximation). The SFG signal is hence predominantly generated by the modes of adsorbed CO, while the centrosymmetric bulk of the Pt crystal and the isotropic gas phase give only a small contribution to the signal.

The source of the visible radiation (790 nm, 2 mJ/pulse, 2 ps, 500 Hz) in our setup was an amplified titanium sapphire laser, and 90% of the output was used to generate tunable infrared light (3−6 μm, ca. 10 μJ/pulse) with an optical parametric generator/amplifier (OPG/OPA). The infrared power was nearly constant between 2000 and 3300 cm^{-1} but decreased below 2000 cm^{-1} due to a reduction of the transmission of the $AgGaS_2$ crystal in the OPG/OPA. The IR frequency was calibrated to an accuracy of $\pm$ 3 cm^{-1} by measurements of the atmospheric CO_2 absorption bands around 2350 cm^{-1}. The IR and visible beams were parallel- (p-) polarized, which predominantly results in a p-polarized output.

2.2. SFG-Compatible UHV−High-Pressure Cell. To meet the requirements of sample preparation and characterization in UHV and of SFG experiments from 10^{-7} mbar to atmospheric pressure, our apparatus was designed as a two-level chamber. Details of the experimental setup were published elsewhere.[11,12] Briefly, the upper level is a UHV surface analysis chamber (base pressure 1×10^{-10} mbar) equipped with low-energy electron diffraction (LEED), Auger electron spectroscopy (AES), and temperature-programmed desorption (TPD). By use of an *xyzφ* manipulator, the sample can be transferred to the lower level where the SFG-compatible reaction cell is situated. The Pt crystal was spot-welded to two Mo rods and could be resistively heated to 1300 K and cooled with liquid N_2 to 85 K (type K thermocouple).

The Pt(111) single-crystal surface, prepared by standard cutting and polishing techniques, was cleaned by repeated Ar ion bombardment (beam energy 1 kV at 2×10^{-4} mbar of Ar) at 300 K for 30 min and subsequent annealing at 1200 K for 3 min. If necessary, oxidation in 10^{-7} mbar of O_2 was used to remove carbon contamination. The surface structure and cleanliness were examined by LEED, AES, and TPD.

For vibrational spectroscopy, the specimen was transferred under UHV to the SFG-compatible reaction cell. When the manipulator is lowered to the SFG level, the sample holder is inserted into an arrangement of three differentially pumped spring-loaded Teflon seals and the SFG cell is separated from the UHV part. Since the SFG cell is pumped by its own turbomolecular pump, the UHV environment is maintained during this operation. The cell is equipped with two CaF_2 windows to allow infrared and visible light to enter and to allow sum frequency light to exit to the detector. The infrared and visible beams make angles of about 55° and 50° with respect to the surface normal. The difference in the incident angles of the beams is necessary to spatially separate the SFG signal from the reflected pump beams. When CO was introduced, the reaction cell could be pressurized up to 1 bar while the upper chamber could still be kept at 5×10^{-10} mbar. CO was introduced via a cold trap filled with a liquid nitrogen/ethanol mixture (ca. 170 K) to remove Ni− and Fe−carbonyl impurities. It should be noted that impurities in the 10^{-4} % range, which can be nearly neglected under UHV conditions, can have a significant partial pressure at high CO pressure (see below). To apply low exposures in UHV experiments, a leak valve and an ionization gauge were also connected to the SFG cell.

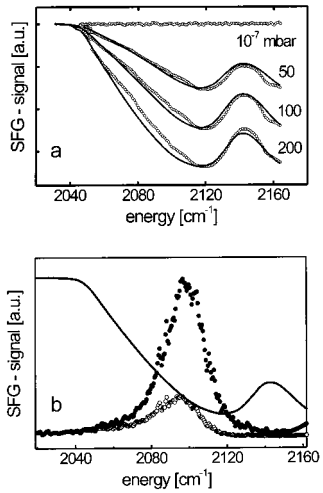

Figure 1. (a) Influence of IR absorption by gas-phase CO on the SFG signal of a GaAs reference crystal located at the sample position. The experimental data points (○) were fitted by use of the Lambert−Beer equation to obtain compensation curves (—). (b) The experimental (raw) SFG spectrum of 200 mbar of CO on Pt(111) at 300 K (○) is plotted together with the corrected spectrum (b) and the corresponding gas-phase compensation curve (—).

3. Results

3.1. IR Absorption by Gas-Phase CO. In principle, the SFG process is independent of pressure because no sum frequency signal is produced by gas-phase CO. However, although the beam length within our SFG cell is less than 5 cm, a significant absorption of infrared light by gas-phase CO occurs at pressures above 1 mbar via vibrational and rotational excitations.[11] Since the number of generated SFG photons depends on the available energy of the incident IR pulse, which in turn is influenced by gas-phase absorption, the SFG process is indirectly influenced by the CO pressure. This is illustrated in Figure 1a, which shows SFG spectra of a GaAs reference crystal at the sample position in 10^{-7}, 50, 100, and 200 mbar CO. Due to its zinc blende structure, GaAs has no inversion symmetry and produces a constant bulk SFG signal in 10^{-7} mbar CO. The variation of the SFG signal at 50, 100, and 200 mbar of CO results from IR gas-phase absorption and the P-branch of the (unresolved) rotational sidebands can be recognized. The experimental traces (○) were fitted to the Lambert−Beer equation, and IR−absorption data from the literature[16] were used to determine an energy-dependent extinction coefficient $\epsilon(E)$. The SFG spectra were normalized by dividing the experimental plots by the corresponding gas-phase absorption curves. In Figure 1b, the raw SFG spectrum of 200 mbar of CO on Pt(111) at 300 K (○) is shown together with the corrected spectrum (b) and the

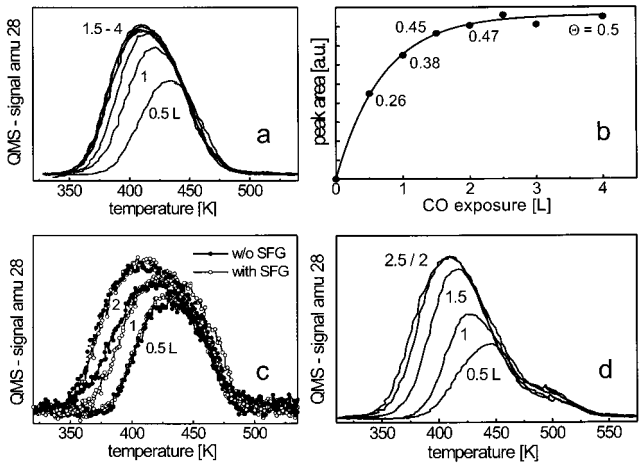

Figure 2. (a) TPD spectra for a series of CO exposures on Pt(111) at 300 K collected at a heating rate of 2 K s^{-1} (exposure indicated in langmuirs). (b) CO uptake curve calculated from the TPD spectra shown in panel a; the saturation coverage at 300 K when CO forms an ordered c(4 × 2) structure with $\theta = 0.5$ was used as reference. (c) TPD spectra for different CO exposures on Pt(111), taken directly after dosing (c) and after sample transfer and subsequent acquisition of an SFG spectrum (○), demonstrating the absence of laser-induced desorption. (d) TPD spectra for different CO exposures on a rough, unannealed Pt(111) surface at 300 K.

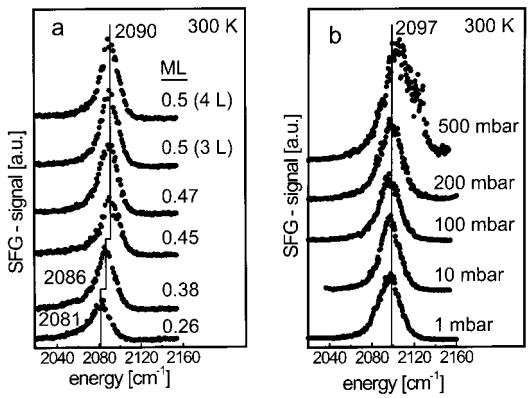

Figure 3. SFG spectra of CO adsorption on Pt(111) at 300 K for submonolayer coverages (a) and in the pressure range from 1 to 500 mbar (b). Spectra above 1 mbar were corrected for CO gas phase absorption. On-top CO was the only species detected (see text).

applied gas-phase compensation curve (—). It should be noted that for our small SFG cell the correction mainly influences the peak area while the peak position is only slightly shifted (from 2094 to 2097 cm^{-1}). By this procedure, all high-pressure SFG spectra shown below were accurately corrected for gas-phase absorption.

3.2. Adsorption of CO on Pt(111) from 10^{-7} to 500 mbar. *3.2.1. Temperature-Programmed Desorption.* To determine the coverage of CO on Pt(111), TPD spectra were acquired for a series of exposures. Figure 2a shows TPD traces after exposures of 0.5−4 langmuirs (1 langmuir = 10^{-6} Torr·s) at 300 K, in increments of 0.5 langmuir. At low coverage (0.5 langmuir) the desorption maximum is found at 435 K, and it shifts to 410 K at the saturation coverage of 4 langmuirs. Figure 2b displays the integrated TPD peak areas vs exposure in langmuirs. At saturation, a well-developed c(4 × 2) structure was observed by LEED, and since the surface coverage of this structure equals 0.5,[17] it was used as reference point to convert exposures to coverages (indicated in Figure 2b). By application of the Redhead formula to approximate the CO adsorption energy (prefactor of 10^{13} s^{-1}), 108 kJ mol^{-1} (1.12 eV) was obtained at saturation coverage (1.20 eV for low θ).

It is apparent that such a calibration is only valid if the coverage is not changed during (or by) SFG spectroscopy. To rule out the possibility of laser-induced photodesorption or thermal desorption of CO, another series of TPD experiments was performed. The Pt(111) surface was exposed to, e.g., 2 langmuirs of CO at 230 K and a TPD spectrum was taken (Figure 2c). Subsequently, the Pt(111) surface was again exposed to 2 langmuirs of CO and transferred to the high-pressure SFG cell. After an SFG spectrum was acquired, the Pt crystal was transferred back in the surface analysis chamber and a second TPD spectrum was measured. As seen in Figure 2c, no change in surface coverage resulting from sample transfer or spectroscopy could be detected under our experimental conditions.

3.2.2. CO Adsorption at 300 and 400 K. Figure 3a displays SFG spectra of CO adsorption on Pt(111) at 300 K for exposures up to 0.5 monolayer (4 langmuirs). The nonlinear response from the clean Pt surface was small but constant over the spectral region shown (less than 5% of the CO signal) and could be easily subtracted. At 0.26 monolayer CO, a single resonance feature at 2081 cm^{-1} was observed, which is characteristic of the C−O stretching vibration of terminally bonded (on-top) CO.[18] With increasing coverage the peak shifted to 2090 cm^{-1} as a result of dynamic dipole coupling, and the SFG peak position and area "saturated" around 0.5 monolayer (ca. 2 langmuirs) coverage (similar to the TPD peak position; cf. Figure 2a,b). Nearly identical CO frequencies and band shifts were reported in an IRAS study by Olsen and Masel.[19] In agreement with previous studies, at saturation coverage a c(4 × 2) LEED pattern was observed,[17] corresponding to a superstructure in which an equal number of CO molecules occupy on-top and bridge sites ($\theta = 0.5$). This adsorption geometry was recently also confirmed by comparison of experimental and simulated STM images.[20] While the resonance frequency of on-top CO agrees well with previous HREELS,[21,22] IRAS,[19,23] and SFG[6,10,24,25] studies, the absence of bridge-bonded CO (expected around 1850 cm^{-1}) in our spectra is probably due to our low IR energy below 1900 cm^{-1}. However, earlier SFG studies of CO on Pt(111) and Pt foil with higher IR energies have also reported difficulties in detecting bridge-bonded CO and attributed this effect to a low Raman polarizability[6,10] and/or an inherently broad line width of bridged CO at room temperature, resulting in a pronounced weakening of the SFG signal.[24] Consequently, in the following we will focus on terminal CO.

The SFG spectrum at 4 langmuirs is identical to a spectrum at 10^{-7} mbar CO. Increasing the pressure to 1, 10, and 100 mbar further shifted the frequency to 2097 cm^{-1} with an ≈40% increase in intensity (Figure 3b). As mentioned in section 3.1, SFG spectra taken at CO pressures >1 mbar were corrected for IR gas-phase absorption. If the maximum value of the (resonant) SFG signal intensity is simply taken as a measure of the on-top CO concentration [again with the c(4 × 2) structure as reference], a CO coverage of about 0.7 is calculated. Although in good agreement with ref 17, this value should be considered an estimate because the SFG intensity depends not only on the adsorbate surface concentration but also on other terms such as the infrared and Raman transition moments.[10,26,27] Increasing the CO pressure to 200 mbar did not further shift the frequency, and on-top CO was the only species detected in a frequency range between 1800 and 2400 cm^{-1} (Figure 3b). SFG spectra recorded up to 500 mbar of CO also showed center peak frequencies around 2100 cm^{-1}. However, the peak width was nearly doubled due to the small signal-to-noise ratio of our

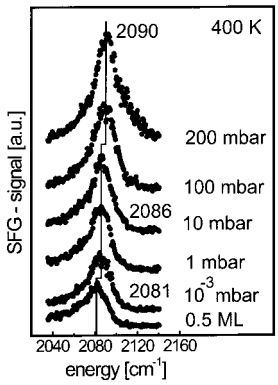

Figure 4. High-pressure CO adsorption on Pt(111) at 400 K monitored by SFG spectroscopy.

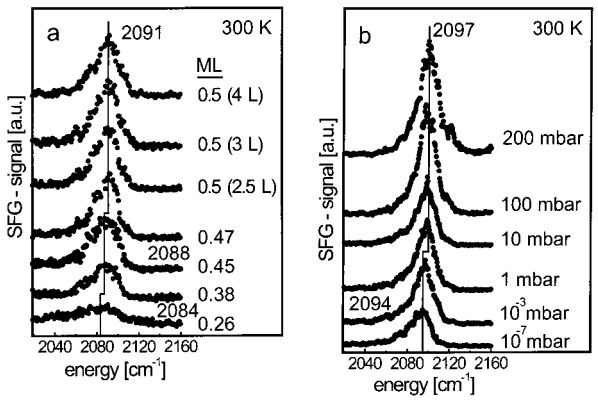

Figure 5. SFG vibrational spectra of CO adsorbed on a defective, unannealed Pt(111) surface at 300 K (cf. Figure 2d): (a) submonolayer range; (b) 10^{-7} to 200 mbar. The spectra are nearly identical to those acquired on the defect-free surface.

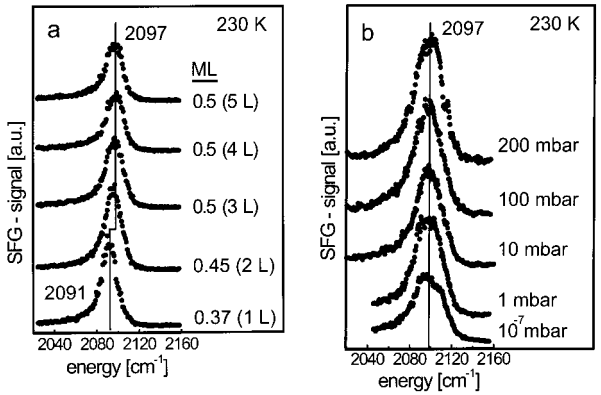

Figure 6. SFG spectra of CO adsorption on Pt(111) at 230 K: (a) submonolayer range; (b) 10^{-7} to 200 mbar of CO.

current SFG setup that prevents an exact gas-phase compensation under these conditions. In the following, we will therefore exclude spectra above 200 mbar of CO.

Our results indicate that the adsorption geometry of CO on Pt(111) at 300 K is independent of gas pressure, in variance to the results of Su et al.,[6] where a decrease of the on-top peak and a new feature around 2050 cm^{-1} was observed above 15 mbar of CO, dominating the spectrum at 150 mbar and higher. Su et al.[6] have attributed the changes in the vibrational spectrum to the formation of carbonyllike Pt−$(CO)_n$ ($n = 1-4$) species. This was accompanied by the formation of an incommensurate CO overlayer around 200 mbar of CO, as also observed by high-pressure STM.[5] Since the presence of an incommensurate CO overlayer should lead to line broadening due to the reduced registry between CO and Pt, the broad 500 mbar peak in Figure 3b might in part originate from such a structure. Härle et al.[10] have carried out a similar study on (polycrystalline) Pt foil and report similar features as in ref 6. The appearance of a new low-frequency CO species was observed above 50 mbar, paralleled by a decrease of the on-top peak intensity above 10 mbar. The low-frequency species dominated the SFG spectra above 300 mbar and was again attributed to platinum−carbonyl binary complexes. However, the intensity of the low-frequency species was only about 2% of the on-top CO signal at 10 mbar of CO.

In light of the absence of these features in our spectra, we have also measured SFG spectra at 400 K, since the formation of carbonyls should be facilitated by higher temperatures. Figure 4 shows SFG spectra taken at 400 K between 0.5 monolayer and 200 mbar of CO. No attenuation or strong red shift of the terminal CO peak was observed with increasing pressure, even after hours of CO exposure. The spectra were identical when measured from low to high or from high to low pressure. The lower frequency of on-top CO at 400 K (2090 cm^{-1}) as compared to the one at 300 K (2097 cm^{-1}) is in good agreement with ref 27 and can be explained by the model of Persson et al.[28,29] With increasing temperature, the stretching frequency of on-top CO shifts toward the frequency of bridged CO due to anharmonic coupling to a frustrated translational mode.

3.2.3. CO Adsorption on Rough Pt(111) at 300 K. The presence of surface defects may also influence a pressure-induced carbonyl formation or a surface reorganization, since defects may act as "nucleation/initiation centers" for this process, as discussed in ref 10. Furthermore, Pt−carbonyls may be preferentially formed at protruding Pt atoms. Such atoms may originate from displacive reconstruction when Pt atoms are pulled out of the surface by CO adsorption, as shown by LEED crystallography.[30] We have therefore deliberately increased the number of defects on Pt(111) by sputtering the surface without subsequent annealing. The high-temperature shoulder around 490 K in the TPD spectra shown in Figure 2d proves the presence of defects and corresponds to a CO adsorption energy of 130 kJ mol^{-1} (1.35 eV). However, SFG spectra of the rough (111) surface acquired at 300 K (Figure 5) were only slightly different from the spectra of the smooth (1×1) face (cf. Figure 3). The only influence of the defects is to generate a low-frequency shoulder that is most pronounced at low coverages. Both SFG and TPD indicate that CO initially adsorbs at step/kink sites and subsequently on the terraces. The observed frequencies are in agreement with related studies on rough and high-index surfaces[24,25,31−33] and also with calculations by Greenler and co-workers[34] that predict that the frequency of on-top CO at a step site to be about 9 cm^{-1} lower than on a terrace site. Nevertheless, on-top CO remained the only species observed.

3.2.4. CO Adsorption at 230 and 160 K. To complete the picture, CO adsorption was also examined at 230 K (Figure 6) but the result was again identical to the spectrum measured at 300 K, except for a small temperature-induced frequency shift at submonolayer coverages.[28] Finally, the sample temperature was lowered to 160 K. In Figure 7, the exposure is indicated in langmuirs because a coverage calibration was not performed. At 160 K, saturation was already achieved at 1 langmuir. For this reason, the CO frequency did not change between 1 and 4 langmuirs (2099 cm^{-1}) and was only slightly changed at 10^{-3} mbar (2101 cm^{-1}). The peaks between 1 and 4 langmuirs exhibit the smallest line width observed in our study (15 cm^{-1}) and are indicative of the resolution of our SFG system.

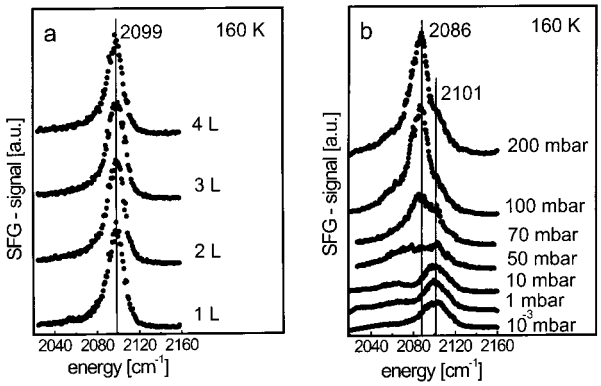

Figure 7. SFG vibrational spectra of CO adsorption on Pt(111) at 160 K: (a) at submonolayer coverage and (b) from 10^{-3} to 200 mbar. Above 10 mbar of CO, a second peak evolved that dominated the spectra at $\geq$70 mbar (it should be noted that a different scale was used for the SFG signal in panels a and b).

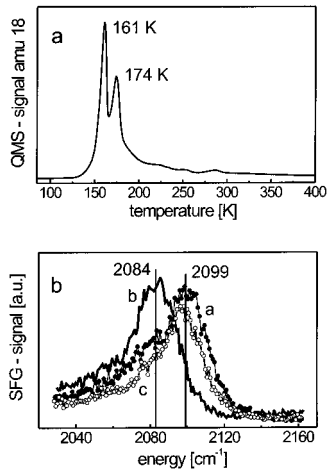

Figure 8. (a) TPD spectrum acquired immediately after the high-pressure SFG spectra of Figure 7b were taken. (b) Coadsorption of CO and water: SFG spectrum taken after an exposure of 5 langmuirs of CO at 160 K (line a), after coadsorption of 5 langmuirs of H_2O (line b), and after increasing the sample temperature to 230 K (line c) (see text).

With increasing CO pressure no change was evident up to 10 mbar of CO, but around 50 mbar a second peak at 2086 cm^{-1} appeared that increased in intensity with pressure. At 200 mbar of CO, its intensity was about 4 times larger than that of the peak at 10 mbar of CO. The frequency of this new peak and, in particular, its appearance at pressures >10 mbar is somewhat reminiscent of the low-frequency features reported in refs 6, 7, and 10. However, in our study the peak at 2086 cm^{-1} could only be observed at 160 K.

As mentioned in section 2.2, at high CO pressure the influence of impurities must be considered. While the cold trap was sufficient to prevent contamination with Ni− and Fe−carbonyls, at high CO pressure it was not able to suppress water traces in the CO feed. This is illustrated by the TPD spectrum in Figure 8a, which was acquired immediately after the high-pressure spectra of Figure 7b were taken (of course, after evacuation to $<10^{-7}$ mbar, sample transfer, and cooling to 90 K). Two water peaks occur in the TPD spectrum that result from H_2O multilayer (161 K) and H_2O monolayer (174 K) desorption.[35,36] Apparently, the coadsorption of CO and (contaminant) water at high CO pressures shifts the on-top CO peak to lower wavenumbers. To model this situation, we deliberately coadsorbed CO and water. Figure 8b shows the SFG spectra taken after an exposure of 5 langmuirs of CO at 160 K (line a), after coadsorbing 5 langmuirs of H_2O (line b), and after increasing the sample temperature to 230 K (line c). In agreement with Figure 7, on-top CO was found at a frequency of 2099 cm^{-1}. The addition of 5 langmuirs of H_2O shifted the frequency by 15 cm^{-1} to 2084 cm^{-1} due to the CO−water interaction (see below), similar to the peak at 2086 cm^{-1} found at high CO pressure (however, no peak at 2099 cm^{-1} remained). A comparable shift was reported in an IRAS study on $CO/D_2O/Pt(111)$.[37] Removal of the water by heating above its desorption temperature shifted the peak back to its original position with only a marginal decrease in intensity.

4. Discussion

On-top CO was the only species detected on Pt(111) from 10^{-7} to 500 mbar and between 160 and 400 K, with only a small influence of the Pt surface roughness. The attenuation of terminal CO as reported in refs 6, 7, and 10 was not evident from our SFG spectra and is probably due to IR gas-phase absorption.[38] We also did not observe a low-frequency species, even though bands at 2050 cm^{-1} should be detectable since this range is nearly unaffected by gas-phase absorption (Figure 1). The coadsorption of water impurities red-shifted the CO frequency to 2085 cm^{-1}, but this effect only occurred at a sample temperature of 160 K. Under these conditions the Pt(111) crystal itself acts as a cold trap and accumulates water. However, at higher temperatures we did not detect any influence from the water impurities and, therefore, the effect of water traces during CO adsorption or oxidation at high temperature (e.g., above 600 K in ref 7) should be negligible.

The adsorption geometry of CO seems to be independent of pressure; i.e., for CO on Pt(111) an extrapolation of UHV data to (high-pressure) catalytic reaction conditions would lead to the correct result (at least for the conditions studied here). However, it should be kept in mind that the adsorption properties of highly dispersed metals may still significantly differ from single-crystal surfaces, as shown in a CO chemisorption study on monodispersed Pt clusters on silica.[39] In fact, we were recently able to demonstrate in an SFG study on alumina-supported Pd nanoparticles (3−6 nm mean size) that the CO adsorption site occupancy (on-top vs bridged CO) strongly depends on the CO pressure, particle size, (surface) structure, and temperature.[11]

The coadsorption of CO and water at 160 K can be explained as follows. Under UHV conditions, the CO saturation coverage is 0.5 monolayer; i.e., there is enough space to accommodate water molecules between the CO molecules (Figure 8b). Water adsorbs via the oxygen and is able to donate electrons to the metal, which results in an increased back-donation between Pt and CO. Such substrate-mediated interactions also occur when CO is coadsorbed with alkali metals.[40] According to the Blyholder model [whose validity was recently supported by a first-principles study of CO on Pt(111)[41]], the C−O bond is weakened and the CO frequency is shifted to lower energy (from 2099 to 2084 cm^{-1} in Figure 8b). If water is subsequently desorbed, this effect is reversed and the CO peak shifts back to its original position.

However, there is a difference between the experiments in UHV (when water was deliberately added) and under high pressure (when water was an impurity in the CO feed). At low pressure the CO peak is simply shifted by coadsorbed water (Figure 8b), while at high pressure a second peak is formed beside the "undisturbed" CO peak (Figure 7b). Several reasons may account for this effect. The simplest explanation is the presence of two domains on the surface, one with pure CO and the other with coadsorbed CO/H_2O. Since it is unclear why two

domains should exist, we favor another explanation. At pressures around 10^{-3} mbar at 160 K, the CO coverage of the Pt surface presumably exceeds 0.7 monolayer and the surface may even be nearly fully covered with CO (while the water concentration is still very small). Consequently, when the CO pressure reaches 50 mbar and the water level becomes significant, the water molecules cannot directly adsorb on the metal surface but only on top of the CO layer where they coadsorb with CO. The strong increase in intensity of the peak at 2086 cm^{-1} above 50 mbar suggests that the growing ice layer incorporates CO in an ordered fashion (but without inversion symmetry). This would explain why the "undisturbed" CO peak remains while the second peak evolves. Further experiments are certainly necessary to understand this phenomenon, but an ordered growth of ice on Pt(111) was reported by the Berkeley group[35] and an IRAS study of $CO/D_2O/Pt(111)$ has shown a strong dependence of water adsorption on the CO coverage.[37] If the gas pressure is reduced below 10^{-4} mbar, part of the multilayers and the CO monolayer desorb, and during this process some of the water is able to readsorb directly on the Pt surface, resulting in a TPD spectrum as shown in Figure 8a.

We have stressed the importance of compensating the IR gas-phase absorption in previous publications.[11,42] As demonstrated in section 3.1, all of our spectra above 1 mbar of CO were corrected accordingly. However, under ideal conditions, part of the visible and IR beams used for the experiment should be split and a reference spectrum of GaAs in the same gas environment should be acquired simultaneously with every SFG spectrum. In this way, variations in laser power, optical alignment, detector sensitivity, etc., could be corrected in addition to the gas-phase absorption. Unfortunately, the small IR energy of the SFG setup used for this study prevented the implementation of such an "on-line" reference.

5. Conclusions

The combination of a surface analysis chamber with an SFG-compatible UHV−high-pressure cell allows the study of adsorbates on well-defined surfaces from submonolayer coverages up to several hundred millibar of gas pressure. Studies of CO adsorption on Pt(111) between 160 and 400 K indicate that CO adsorbs on on-top sites, independent of gas pressure from 10^{-7} mbar (0.25 monolayer) to 500 mbar. No evidence for pressure-induced changes or for a high-pressure "low-frequency" CO species was found. The absence of bridge-bonded CO in the SFG spectra is due to the small sensitivity of SFG for this particular adsorbate/substrate combination. The coadsorption of CO and water at 160 K resulted in a red shift of the CO peak due to electron donation from water to Pt. When high-pressure experiments (>1 mbar) are carried out, great care has to be taken to control impurities that can be generally neglected under UHV conditions. We are currently setting up a new OPG/OPA system that will significantly increase the IR energy below 2000 cm^{-1}, improve the resolution to 5 cm^{-1}, and allow the implementation of a reference cell. SFG studies carried out during catalytic reactions are in progress.

References and Notes

(1) Thomas, J. M.; Thomas, W. J. *Principles and Practice of Heterogeneous Catalysis*; VCH: Weinheim, Germany, 1997.
(2) Somorjai, G. A. *Introduction to Surface Chemistry and Catalysis*; John Wiley & Sons: New York, 1994.
(3) Ertl, G.; Freund, H.-J. *Phys. Today* **1999**, *52*, 32.
(4) Yates, J. T. *Surf. Sci.* **1994**, *299/300*, 731.
(5) Jensen, J. A.; Rider, K. B.; Salmeron, M.; Somorjai, G. A. *Phys. Rev. Lett.* **1998**, *80*, 1228.
(6) Su, X.; Cremer, P. S.; Shen, Y. R.; Somorjai, G. A. *Phys. Rev. Lett.* **1996**, *77*, 3858.
(7) Su, X.; Cremer, P. S.; Shen, Y. R.; Somorjai, G. A. *J. Am. Chem. Soc.* **1997**, *119*, 3994.
(8) Su, X.; Jensen, J.; Yang, M. X.; Salmeron, M.; Shen, Y. R.; Somorjai, G. A. *Faraday Discuss.* **1996**, *105*, 263.
(9) McIntyre, B. J.; Salmeron, M.; Somorjai, G. A. *Rev. Sci. Intrum.* **1993**, *64*, 687.
(10) Härle, H.; Metka, U.; Volpp, H.-R.; Wolfrum, J. *Phys. Chem. Chem. Phys.* **1999**, *1*, 5059.
(11) Dellwig, T.; Rupprechter, G.; Unterhalt, H.; Freund, H.-J. *Phys. Rev. Lett.* **2000**, *85*, 776.
(12) Rupprechter, G.; Dellwig, T.; Unterhalt, H.; Freund, H.-J. *Stud. Surf. Sci. Catal.* **2000**, *130*, 3131.
(13) Shen, Y. R. *Nature* **1989**, *337*, 519.
(14) Miragliotta, J.; Rabinowitz, P.; Cameron, S. D.; Hall, R. B. *Appl. Phys. A* **1990**, *51*, 221.
(15) Shen, Y. R. *Surf. Sci.* **1994**, *299/300*, 551.
(16) Schrader, B. *Raman/Infrared Atlas of Organic Compounds*; VCH: Weinheim, Germany, 1989.
(17) Ertl, G.; Neumann, M.; Streit, K. M. *Surf. Sci.* **1977**, *64*, 393.
(18) Sheppard, N.; Nguyen, T. T. *Adv. Infrared Raman Spectrosc.* **1978**, *5*, 67.
(19) Olsen, C. W.; Masel, R. I. *Surf. Sci.* **1988**, *201*, 444.
(20) Pedersen, M. O.; Bocquet, M.-L.; Sautet, P.; Laegsgaard, E.; Stensgaard, I.; Besenbacher, F. *Chem. Phys. Lett.* **1999**, *299*, 403.
(21) Avery, N. R. *J. Chem. Phys.* **1981**, *74*, 4202.
(22) Steininger, H.; Lehwald, S.; Ibach, H. *Surf. Sci.* **1982**, *123*, 264.
(23) Hayden, B. E.; Bradshaw, A. M. *Surf. Sci.* **1983**, *125*, 787.
(24) Klünker, C.; Balden, M.; Lehwald, S.; Daum, W. *Surf. Sci.* **1996**, *360*, 104.
(25) Härle, H.; Mendel, K.; Metka, U.; Volpp, H. R.; Willms, L.; Wolfrum, J. *Chem. Phys. Lett.* **1997**, *279*, 275.
(26) Somorjai, G. A.; Rupprechter, G. *J. Phys. Chem. B* **1999**, *103*, 1623.
(27) Härle, H.; Lehnert, A.; Metka, U.; Volpp, H. R.; Willms, L.; Wolfrum, J. *Appl. Phys. B* **1999**, *68*, 567.
(28) Persson, B. N. J.; Ryberg, R. *Phys. Rev. B.* **1985**, *32*, 3586.
(29) Persson, B. N. J.; Hoffmann, F. M.; Ryberg, R. *Phys. Rev. B.* **1989**, *34*, 2266.
(30) Wander, A.; Van Hove, M. A.; Somorjai, G. A. *Phys. Rev. Lett.* **1991**, *67*, 626.
(31) Härle, H.; Lehnert, A.; Metka, U.; Volpp, H. R.; Willms, L.; Wolfrum, J. *Chem. Phys. Lett.* **1998**, *293*, 26.
(32) Hollins, P. *Surf. Sci. Rep.* **1992**, *16*, 51.
(33) Hayden, B. E.; Kretzschmar, K.; Bradshaw, A. M.; Greenler, R. G. *Surf. Sci.* **1985**, *149*, 394.
(34) Leibsle, F. M.; Sorbello, R. S.; Greenler, R. G. *Surf. Sci.* **1987**, *179*, 101.
(35) Su, X.; Lianos, L.; Shen, Y. R.; Somorjai, G. A. *Phys. Rev. Lett.* **1998**, *80*, 1533.
(36) Thiel, P. A.; Madey, T. D. *Surf. Sci. Rep.* **1987**, *7*, 211.
(37) Ogasawara, H.; Yoshinobu, J.; Kawai, M. *Surf. Sci.* **1997**, *386*, 73, and references therein.
(38) Private communication: The Berkeley group has confirmed the presence of on-top CO up to 400 mbar at 300 K, using a smaller SFG cell that minimizes gas-phase absorption. See also Kung, K. Y.; Chen, P.; Wei, F.; Shen, Y. R.; Somorjai, G. A. *Surf. Sci. Lett.* **2000**, *463*, L627.
(39) Heiz, U.; Sherwood, R.; Cox, D. M.; Kaldor, A.; Yates, J. T. *J. Phys. Chem.* **1995**, *99*, 8730.
(40) Bonzel, H. P. *Surf. Sci. Rep.* **1987**, *8*, 43.
(41) Aizawa, H.; Tsuneyuki, S. *Surf. Sci.* **1998**, *399*, L364.
(42) Rupprechter, G.; Dellwig, T.; Unterhalt, H.; Freund, H.-J. *Top. Catal.* **2001**, *15*, 19.